Journal of Catalysis **209,** 331–340 (2002)
doi:10.1006/jcat.2002.3642

Vapor-Phase Epoxidation of Propene Using H_2 and O_2 over Au/Ti–MCM-48

B. S. Uphade, T. Akita, T. Nakamura, and M. Haruta[1,2]

Osaka National Research Institute, AIST, Midorigaoka 1-8-31, Ikeda 563-8577, Japan

Received August 16, 2001; revised April 8, 2002; accepted April 23, 2002

Vapor-phase epoxidation of propene using H_2 and O_2 over homogeneously dispersed gold particles deposited by a deposition–precipitation (DP) method on the supports Ti–MCM-41 (hexagonal) and Ti–MCM-48 (cubic) is studied at a space velocity of 4000 $h^{-1} \cdot cm^{-3}$/g(cat.) and at reaction temperature of 100 or 150°C. Influences of the various parameters investigated in the case of Ti–MCM-48 support are Si/Ti (30, 50, 75, and 100) ratios, precipitating agents (LiOH, NaOH, KOH, RbOH, or CsOH) for Au deposition, pH (6–8), Au loading (2–25 wt% in solution), and calcination temperature (150–500°C). The supports were characterized by XRD, UV–vis, FT-IR, and surface area measurements, whereas supported gold catalysts were characterized by TEM, ICP, and XPS techniques. Better performance was observed with Ti–MCM-48 (initial conversion = 5.6%, PO selectivity = 92%), due to its three-dimensional pore system, than with Ti–MCM-41 (initial conversion = 5.1%, PO selectivity = 88%) in the propene epoxidation at 150°C. GC–MS investigation of the extracted species using organic solvent from the used catalyst revealed that acidic as well as oligomeric species accumulated on the catalyst surfaces. These species are assumed to cause the catalyst deactivation. Silylation of the catalyst Au/Ti–MCM-48 prohibits it from getting deactivated faster and also helps to improve PO selectivity and decrease H_2 consumption. Based on the above experimental results, a probable reaction mechanism is explained. © 2002 Elsevier Science (USA)

Key Words: **epoxidation; propene; propene oxide; gold; Ti–MCM-41; Ti–MCM-48.**

1. INTRODUCTION

Propene oxide (PO), which is also known by other names, such as propylene oxide, methyl oxirane, and 1,2-epoxypropane, is an important building block for the manufacture of polyurethane, organic intermediates, and solvents. Industrially PO is produced using two commercial processes. These are the chlorohydrin process and the hydroperoxide process (1). The chlorohydrin process is not environmentally friendly, as it produces chlorinated organic by-products as well as calcium chloride, $CaCl_2$. All the recently built plants for the commercial production of PO are, therefore, based on hydroperoxide processes. The disadvantage of the hydroperoxide process is, however, the production of equimolar amounts of the coproduct, either styrene or *tert*-butanol, depending on which variant of hydroperoxide is used in the process.

In the past, extensive efforts have been made to develop an alternative direct gas-phase epoxidation process similar to that for the epoxidation of ethene (2). However, there has so far been no alternative process developed, probably due to low yields, low raw-material conversion, low productivities, numerous by-products, and complex catalyst systems. One of the most important heterogeneous catalysts, CsCl-promoted Ag/Al_2O_3, which is used in the epoxidation of ethylene, could not be used for higher olefins containing allylic hydrogen. This is mainly due to the easy abstraction of methyl hydrogen giving allylic intermediates, leading to direct combustion, thereby lowering PO selectivity. Recently Enichem utilized TS-1 (MFI) as a catalyst for the epoxidation of propene in the liquid phase using hydrogen peroxide (3–5). However, due to the very high production cost of H_2O_2 and its handling problems it is desirable to have the H_2O_2 produced *in situ*. Toso Co. Ltd. (6) has developed Pd/TS-1 catalyst for the *in situ* generation of H_2O_2 from H_2 and O_2. Recently Hölderich and co-workers (7) modified the catalyst developed by Toso with platinum and reported that the improved yield of PO could be ascribed to the maintenance of palladium in its +2 oxidation state.

Our research work on the catalysis of gold (8–10) has opened a new stage for the direct epoxidation of propene using hydrogen and oxygen. We have reported recently, in a series of papers, on the vapor-phase epoxidation of propene over highly dispersed nanosize Au particles supported on TiO_2 (11, 12), TiO_2/SiO_2 (11, 12), and titanosilicates such as TS-1, TS-2, Ti-β, and Ti–MCM-41 (13, 14). This finding is now being followed by a few other researchers (15–17) and companies (18, 19). We reported recently on the formation of propanal from propene, H_2, and O_2 at high temperatures (≥200°C) (20). Recent findings from our group (21) also showed the promoting effect of CsCl when physically mixed with Au/Ti–MCM-41 for the effective utilization of hydrogen.

[1] To whom correspondence should be addressed. Fax: +81-298-61-8240. E-mail: m.haruta@aist.go.jp.

[2] Present address: Research Institute for Green Technology, AIST, Onogawa 16-1, Tsukuba 305-8569, Japan.

0021-9517/02 $35.00
© 2002 Elsevier Science (USA)
All rights reserved.

Here, we report on the epoxidation of propene over Au supported on Ti–MCM-48 (cubic). We already have reported, in a detailed study, on the use of Au/Ti–MCM-41 in propene epoxidation (22). New results on the epoxidation of propene over Au/Ti–MCM-41 (Si/Ti = 67), which were additional to and different from those reported earlier, are included in this paper for comparison purposes. In the family of M41S materials, first reported by Mobil in 1992 (23, 24), MCM-41 (hexagonal arrangement of unidirectional pores indexed in the space group *p6m*) and MCM-48 (cubic structure indexed in the space group *Ia3d*) are very widely studied, both as such and when substituted with redox metals such as Ti and V (25). Earlier studies on gas-phase epoxidation of propene over Au/Ti–MCM-41 (22) showed the fast catalyst deactivation, partly due to the monodimentional array of pores in MCM-41. In accordance with previous reports (26, 27) we are of the opinion that MCM-48, due to its three-dimentional, branched-pore system, would be more resistant to clogging than MCM-41, which has straight channels. It is, therefore, the aim of this study to compare propene epoxidation over Au supported on Ti–MCM-41 and Ti–MCM-48, with emphasis on the latter system. Various factors affecting catalyst activity/selectivity in the support Ti–MCM-48, such as Si/Ti ratio, precipitating agent, and pH for Au deposition, Au loading, and calcination temperature, are discussed in detail. Possible causes of catalyst deactivation, use of silylation to avoid faster catalyst deactivation, and probable reaction mechanisms are also discussed.

2. EXPERIMENTAL

2.1. Synthesis of Hexagonal Ti–MCM-41 Support

Ti–MCM-41 with a Si/Ti atomic ratio of 67 was synthesized according to the patent procedure (28). The molar composition subjected to hydrothermal synthesis used was as follows: SiO_2, $0.015TiO_2$, 0.75CTMACl, 0.27TMAOH, and $71.8H_2O$. In a typical synthesis, 40.6 g tetraethylorthosilicate (TEOS) and 1.0 g tetrabutylammoniumtitanate (TBOT) were hydrolyzed at 80°C for 5 h in N_2 atmosphere under continuous stirring. After cooling to close to room temperature, 47 g of a structure-directing organic template, cetyltrimethylammonium chloride (CTMACl), was added and the mixture was dissolved in 115 ml of 2-propanol (IPA). That mixture was stirred for 1 h and then a mixture of 10 g tetramethylammonium hydroxide (TMAOH, 25% aq.) and 35 ml IPA was added dropwise under vigorous stirring. This mixture was stirred overnight. Finally the remaining 8.9 g TMAOH and 252 g water were added and the mixture was heated to 50°C and kept at this temperature for 8–10 h or until the disappearance of the IPA. After the water content was adjusted, the resulting mixture was transferred to a thick teflon bottle and heated at 100°C under autogeneous pressure and static conditions for 10 days. The product was collected by centrifugation, washed repeatedly with water, dried at 100°C overnight, and finally calcined at 540°C for 6 h in static air.

2.2. Synthesis of Cubic Ti–MCM-48 Support

Ti–MCM-48 with various Si/Ti ratios was synthesized under hydrothermal conditions at 100°C in a static teflon bottle for 10 days according to the literature procedure (29). A typical two-step method for its synthesis is as follows. To a 44% solution of TEOS in IPA, CTMAOH in methanol and water (water/methanol molar ratio = 2) was added to partly hydrolyze TEOS at about 2–5°C. After 1 h, the IPA solution of TBOT was added to the resultant mixture very slowly under vigorous stirring. The mixture was then stirred for 1 h, when the aqueous solution of CTMACl was finally added. The mixture was heated to 50°C for about 6–8 h to remove IPA. The molar composition of the gel subjected to hydrothermal synthesis (100°C, 10 days) was as follows: SiO_2, $xTiO_2$, 1.2CTMAOH, 0.7CTMACl, and $46.6H_2O$, where $x = 0.01$–0.03, Si/CTMA = 1.0, and CTMACl/OH = 70/30.

2.3. Deposition of Au onto Supports

Nanoparticles of Au were deposited on the supports Ti–MCM-41 and Ti–MCM-48 by a deposition–precipitation (DP) method as described previously (30). In a typical catalyst preparation condition an aqueous solution of $HAuCl_4 \cdot 4H_2O$, 0.17 g (8 wt% Au with respect to support), in 200 ml H_2O was heated to 70°C and the pH was adjusted to 7.0 ± 0.1 using an aqueous alkali hydroxide solution. The support, weighing 1.0 g, was suspended to it, the pH was adjusted once again to the same value, and the solution was aged at the above temperature for 1 h. The suspension was washed several times with distilled water, dried at 100°C for 2 h, and finally calcined in air at 300°C for 4 h.

2.4. Characterization of the Supports and Gold Catalysts

The supports, Ti–MCM-41 and Ti–MCM-48, were characterized by XRD (Rigaku Rint-2400, Cu-$K\alpha$ radiation, 40 kV, 40 mA), UV–vis (Photal Otsuka Electronics, MC-2530 UV/vis light source), FT-IR (Nicolet Model 205, KBr pellets containing 1% finely powdered support pressed at 6 tons/cm^2), and specific surface area (Quantasorb Jr.) measurements to confirm the product identity reported in the literature (31–34). Nitrogen adsorption isotherms at −196°C were obtained using a Micromeritics ASAP 2010 volumetric adsorption analyzer. Transmission electron microscopy (TEM) observations were made using a Hitachi H-9000 to determine Au particle size and distribution. XPS (Shimadzu ESCA-KM) was used to determine the electronic state of Au particles and the catalyst's surface. Actual Au and Ti contents in the catalysts were analyzed by an inductively coupled plasma (ICP) technique.

2.5. Catalytic Activity Measurements

Catalytic tests were carried out in a vertical fixed-bed U-shaped quartz reactor (i.d., 10 mm) using a feed containing 10 vol% each C_3H_6, H_2, and O_2 diluted with Ar passed over the catalyst (0.5 g) bed at a space velocity of 4000 $h^{-1} \cdot cm^{-3}$/g catalyst. The temperature was controlled and measured using a glass-tube-covered Cr–Al thermocouple located in the center of the catalyst bed. Prior to testing, the catalysts were first pretreated at 250°C for 30 min in a stream of 10 vol% H_2 in Ar, followed by 10 vol% O_2 in Ar. In the catalytic tests for the samples calcined at different temperatures, from 150–500°C, the pretreatment was carried out only in a stream of 10 vol% O_2 in Ar. The feed and products were analyzed using three online GCs equipped with TCD (AC and porapak Q columns) and FID (HR-20M column) detectors equipped with automatic injection systems. Since the conversions of propene tended to decrease during catalytic activity measurements (see Fig. 6), in principle, the conversions at 30 min after the start of the reactant gas feed are presented in this paper.

Trimethylsilylation (35) of Au/Ti–MCM-48 (Si/Ti = 50) at 150°C was carried out using methoxytrimethyl silane. Silylation was performed as per the patent procedure (36). Methoxytrimethyl silane was kept at 0°C and argon was bubbled at the flow rate of 25 ml/min through the silylating solution for 15 min. The catalyst was then flushed with pure argon for about 5 h at 200°C before the catalytic tests were carried out.

3. RESULTS AND DISCUSSION

3.1. Characterization of Supports and Supported Au Catalysts

3.1.1. N_2 adsorption isotherms. Nitrogen adsorption isotherms for Ti–MCM-41 support are explained in a previous paper (22). For Ti–MCM-48 the isotherms are shown in Figs. 1a and 1b for Si/Ti ratios of 30 and 100, respectively. The isotherms of type IV, typical of mesopore materials, with H2 hysteresis, are observed. At the relative pressure near P/P_0 0.15–0.25, the isotherm exhibits the inflection characteristic of capillary condensation within the mesopores (37). The BJH cumulative surface area, pore volume, and pore diameter for Si/Ti = 50 were 1649 m^2 g^{-1}, 1.3 cm^3 g^{-1}, and 3.24 nm, respectively, whereas for Si/Ti = 30 the values were 1053 m^3 g^{-1}, 0.76 cm^3 g^{-1}, and 2.88 nm, respectively.

3.1.2. XRD, UV–vis, and FT-IR. XRD and UV–vis spectra for the supports Ti–MCM-41 and Ti–MCM-48 are compared in Figs. 2 and 3, respectively. Samples give relatively well-defined XRD patterns typical of MCM-41 and MCM-48 materials, as reported in the literature (31–34). XRD peaks can be indexed on a hexagonal lattice for Ti–MCM-41 and on a cubic lattice for Ti–MCM-48 with

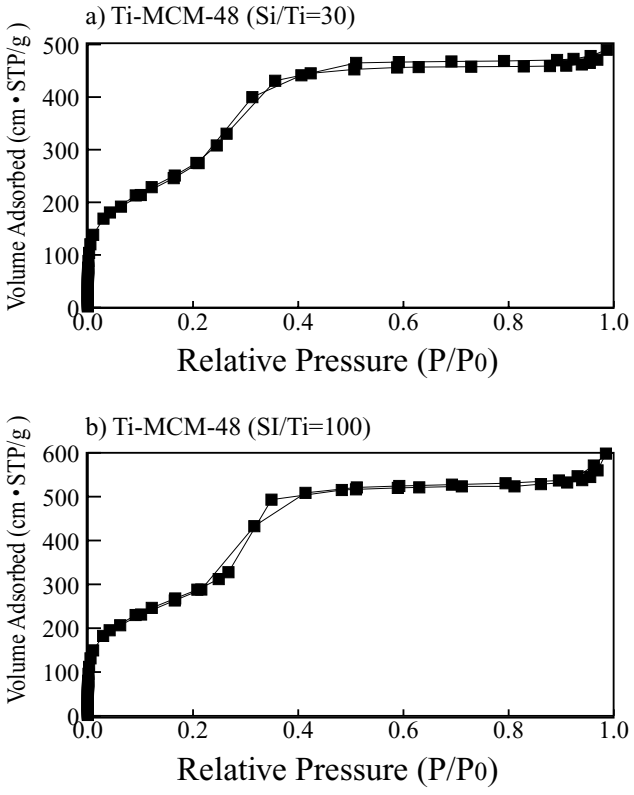

FIG. 1. Nitrogen adsorption–desorption isotherm at −196°C for Ti–MCM-48. (a) Si/Ti = 30; (b) Si/Ti = 100.

pore diameters in the range of ca. 37–40 Å, as shown in Table 1. Ti–MCM-41 exhibits a well-defined (1 0 0) reflection; that and Ti–MCM-48 (2 1 1) and (2 2 0) reflections can be seen in Fig. 2. UV–vis confirmed the absence of a

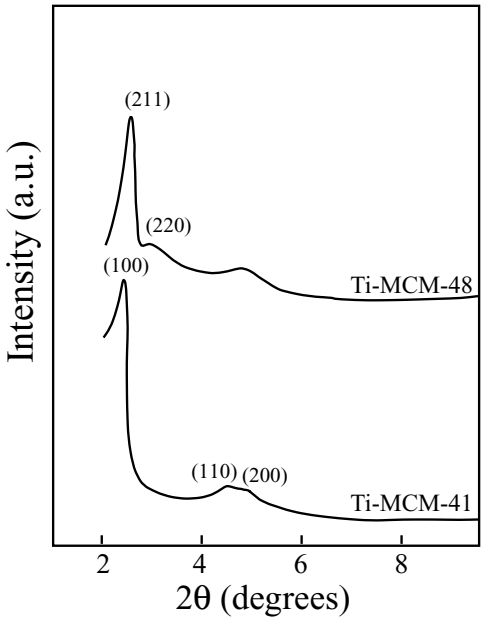

FIG. 2. XRD spectra of Ti–MCM-41 and Ti–MCM-48.

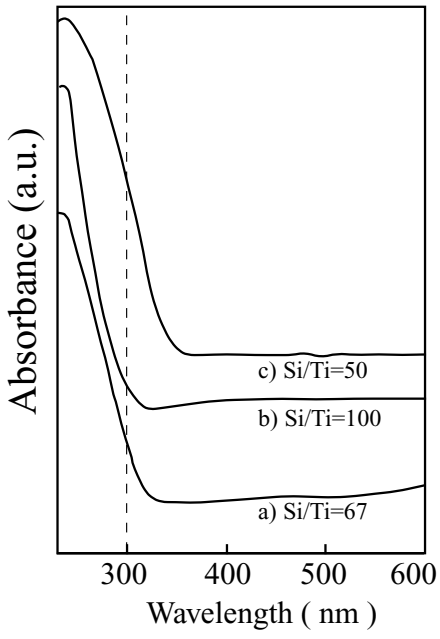

FIG. 3. UV–vis spectra of Ti–MCM-41 [(a) Si/Ti = 100/1.5] and Ti–MCM-48 [(b, c) Si/Ti = 50 and 100].

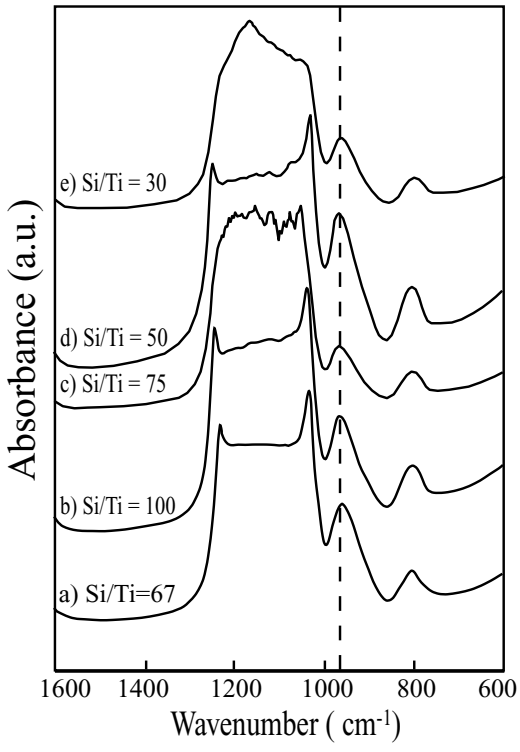

FIG. 4. FT-IR spectra of Ti–MCM for different Si/Ti ratios. (a) Ti–MCM-41; (b–e) Ti–MCM-48.

segregated TiO_2 phase at ca. 330 nm for supports with a titanium content $\leq$2.0 wt%. According to the literature (31, 32) the band at 210 nm is assigned to Ti in tetrahedral coordination whereas the band in the range 270–330 nm is assigned to the Ti in its octahedral coordination. The broad wavelength peak for curve c in Fig. 3 may be indicative of Ti in a distorted tetrahedral environment and the presence of Ti in polymeric octahedral coordination is also possible for this material.

FT-IR spectra (Fig. 4) showed the presence of sharp peak at 963 cm^{-1} indicative of Ti in its tetrahedral coordination

TABLE 1

Preparation Conditions and Characterization of Gold Supported on Hexagonal Ti–MCM-41 and Cubic Ti–MCM-48

Support	Si/Ti ratio	Pore[a] diameter (Å)	Surface area ($m^2 \cdot g^{-1}$)	Au (in soln.) (wt%)	Ppting agent	pH	Loading (wt%) by ICP		D_{AU}[b] (nm)
							Au	Ti	
Ti–MCM-41	67	37.1	970	12	NaOH	7.0	0.42	1.14	2.1
Ti–MCM-48	100	39.1	1117	8	NaOH	7.0	0.04	n.d.[c]	2.3
Ti–MCM-48	75	39.2	n.d.	8	NaOH	7.0	0.06	n.d.	n.d.
Ti–MCM-48	50	39.4	1127	2	NaOH	7.0	0.01	1.10	n.d.
Ti–MCM-48	50	39.4	1127	8	NaOH	7.0	0.09	1.12	2.2
Ti–MCM-48	50	39.4	1127	12	NaOH	7.0	0.11	1.15	n.d.
Ti–MCM-48	50	39.4	1127	16	NaOH	6.0	n.d.	n.d.	2.6
Ti–MCM-48	50	39.4	1127	16	NaOH	7.0	n.d.	n.d.	4.7[d]
Ti–MCM-48	50	39.4	1127	16	KOH	7.0	n.d.	n.d.	2.4
Ti–MCM-48	50	39.4	1127	16	NaOH	8.0	0.11	1.15	2.0
Ti–MCM-48	50	39.4	1127	24	NaOH	7.0	0.30	1.11	n.d.
Ti–MCM-48	50	39.4	1127	16	NaOH	7.0	n.d.	n.d.	2.0
Ti–MCM-48	50	39.4	1127	16	LiOH	7.0	0.07	1.00	2.3
Ti–MCM-48	50	39.4	1127	16	CsOH	7.0	0.35	1.13	2.3
Ti–MCM-48	30	39.3	n.d.	8	NaOH	7.0	0.32	n.d.	n.d.

[a] By XRD.
[b] A deviation of ±1–3 nm is observed.
[c] n.d. = not determined.
[d] Final catalyst calcined at 150°C.

(22). However, as reported elsewhere (32) the peak at 963 cm^{-1} could also be assigned to Si–OH groups in addition to Ti–O–Si bonds and, hence, we calcined materials (MCM-41, MCM-48, Ti–MCM-41, and Ti–MCM-48) at higher temperature. The peak at 963 cm^{-1} disappeared for MCM-41 and MCM-48 but was maintained for Ti–MCM when calcined at 1000°C. The disappearance of the band in pure silicious MCM-41 and MCM-48 when calcined at higher temperature may be attributed to the loss of silanol groups, as reported previously (22). Moreover, the intensity of the peak at 963 cm^{-1}, assumed to be due to silanol groups, clearly shows an increase in its intensity when titanium is present in MCM-41 and MCM-48. Thus, it is clear from our earlier (22) and present study that the major part of titanium is present in the tetrahedral coordination.

3.1.3. ICP and TEM. Actual Au loading by ICP analysis was very small in comparison with the Au content in the DP solution especially on Ti–MCM-48 (Table 1). TEM observations showed a homogeneous dispersion of Au with an average particle size of 2.0–2.6 nm for Au/Ti–MCM-41 and Au/Ti–MCM-48. Typical TEM images of the Au supported on Ti–MCM-41 and Ti–MCM-48 are compared in Figs. 5a and 5b, respectively, whereas the size distributions of Au particles are shown in Figs. 6a and 6b. Average sizes of Au particles calculated for various samples are given in Table 1. It may be noted from Table 1 that the Ti–MCM-48 with a cubic structure deposits less Au loading than hexagonal Ti–MCM-41.

3.2. Epoxidation of Propene over Au/Ti–MCM Catalysts

The results of propene epoxidation at 150°C over Au/Ti–MCM-41 and Au/Ti–MCM-48 are compared in Fig. 7. For both catalysts the initial propene conversion is about 5% and it decreases with time. The superior performance of Au/Ti–MCM-48 in terms of activity, PO selectivity, and also H_2 efficiency over that of Au/Ti–MCM-41 can be attributed to its three-dimensional pore system, which should be more resistant to blockage by extraneous materials like oligomers of PO than the one-dimensional pore system of Ti–MCM-41. Koyano and Tatsumi (29) also have shown in the liquid-phase epoxidation of cyclododecene with H_2O_2 the higher activity of Ti–MCM-48 over that of Ti–MCM-41. Anpo *et al.* (37) also reported higher photocatalytic activity for Ti–MCM-48 than for Ti–MCM-41 in the reduction of CO_2 with H_2O to CH_3OH and concluded that the large pore size and three-dimentional channel structure of MCM-48 results in better dispersion of titanium dioxide and thus the better results.

The results of the influence of Si/Ti ratio in Ti–MCM-48 on the epoxidation of propene over 8% Au/Ti–MCM-48 at

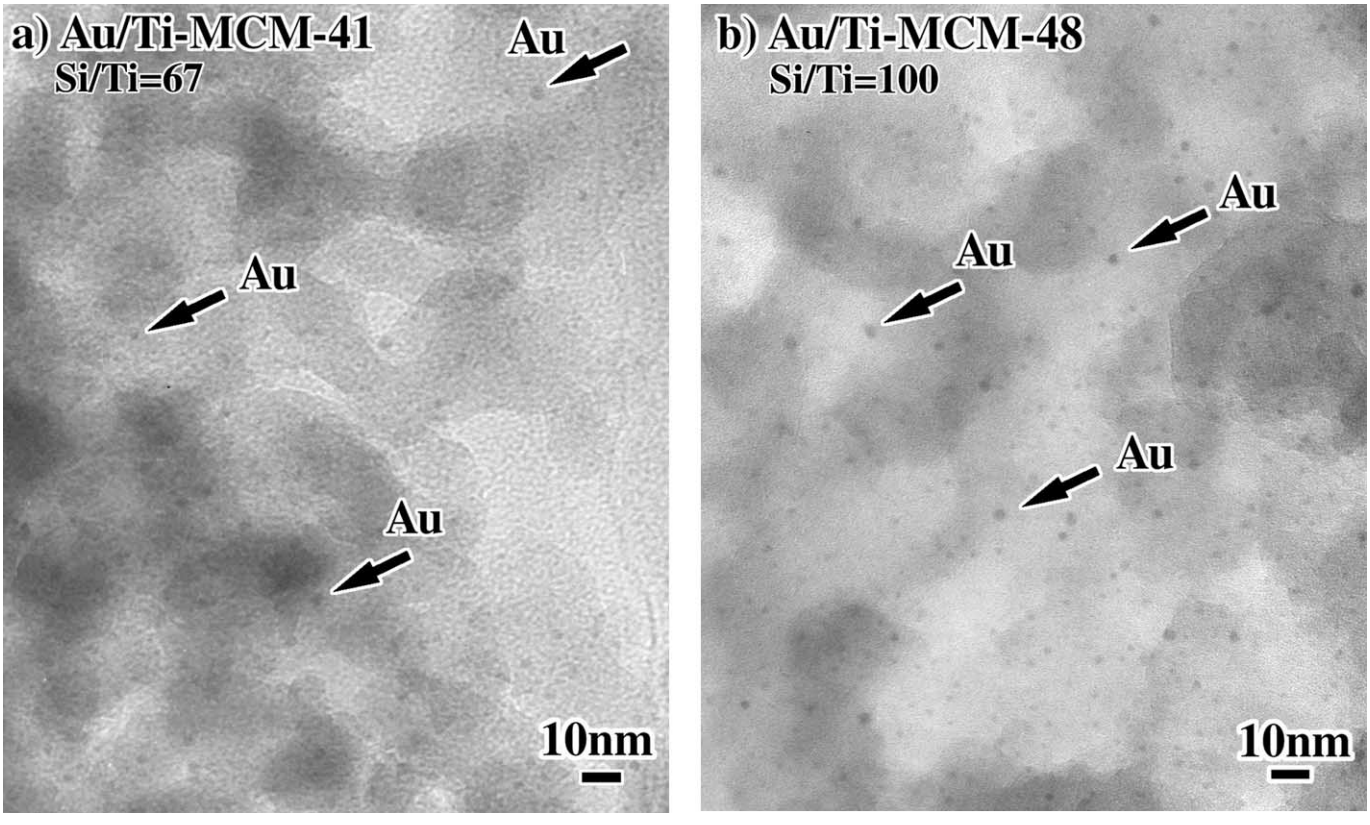

FIG. 5. TEM of (a) Au/Ti–MCM-41 and (b) Au/Ti–MCM-48.

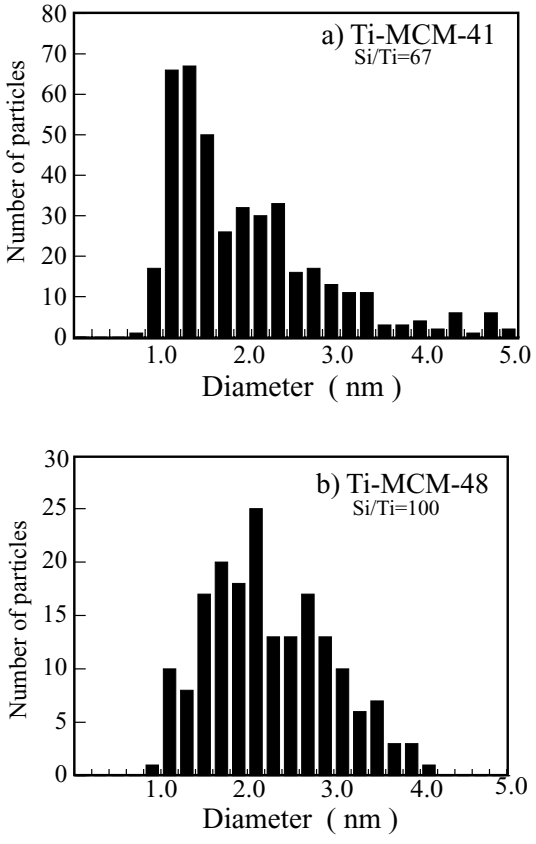

FIG. 6. Size distribution of Au particles supported on (a) Ti–MCM-41 and (b) Ti–MCM-48.

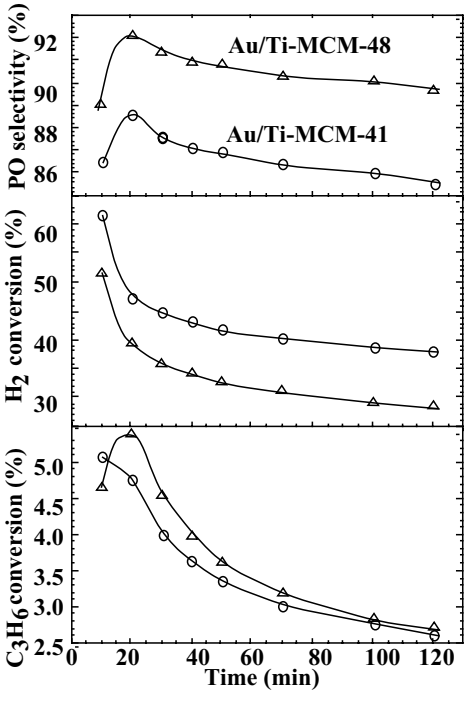

FIG. 7. Influence of support (Ti–MCM-41 vs Ti–MCM-48) in the epoxidation of propene. Au in solution, 12 wt%; temperature, 150°C.

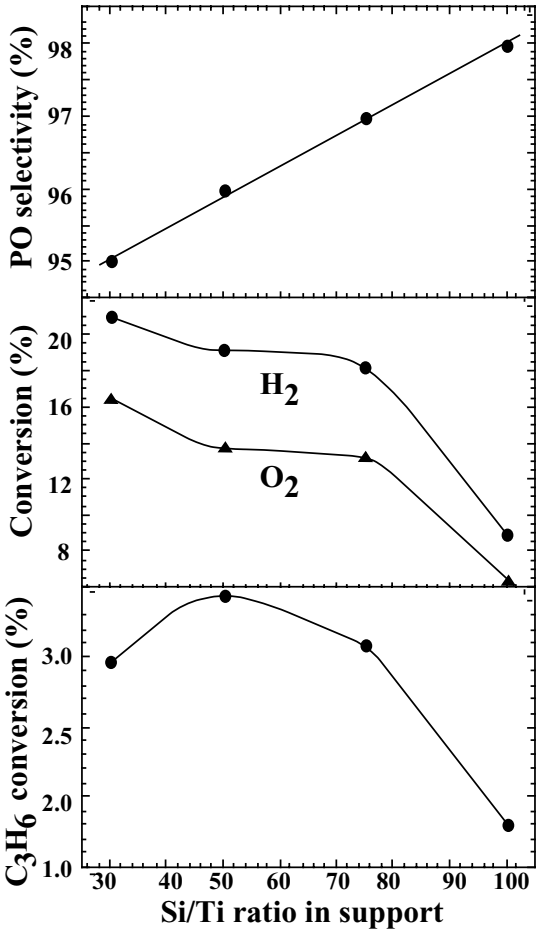

FIG. 8. Influence of Si/Ti ratio in Ti–MCM-48 on the epoxidation of propene over 8 wt% Au/Ti–MCM-48 at 100°C.

100°C are given in Fig. 8. The conversion of H_2 and O_2 decreases whereas PO selectivity increases with an increase in Si/Ti ratio. This can be ascribed to the decrease in Au loading with an increase in Si/Ti ratio due to lower Ti content, as shown in Table 1. The propene conversion passes through a maximum at a Si/Ti ratio of 50. Along similar lines, we reported earlier for Au/Ti–MCM-41 an increase in Au loading on Ti–MCM-41 with a decrease in Si/Ti atomic ratio and hence poor PO selectivity at very high Ti and Au loadings (please see Table 1 and Fig. 11 of Ref. 22). A further decrease in Si/Ti ratio causes a decrease in propene conversion, which is most probably due to the presence of a polymeric anatase TiO_2 phase, as observed by UV–vis and TEM. We have also found that the best results in propene epoxidation are obtained when NaOH is used as a precipitating agent for depositing gold on the supports. The results are presented in Fig. 9. One probable reason for this could be uniform and high dispersion of Au nanoparticles coupled with traces of alkali content. The more basic nature of Na compared with that of Cs may be another reason for higher PO selectivity. It should also be noted from Table 1 that the

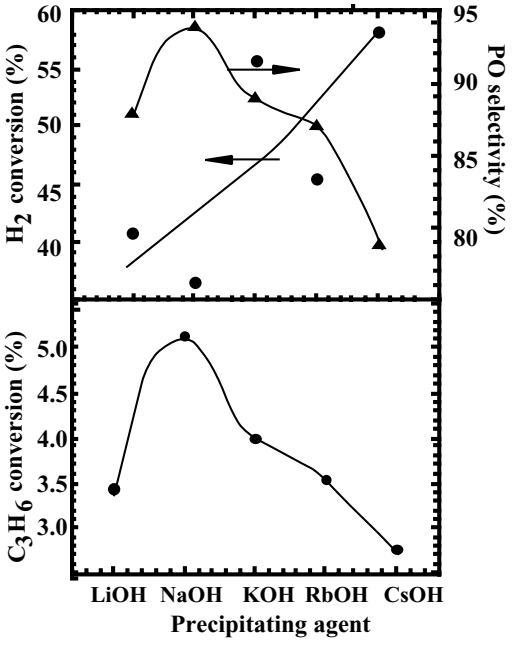

FIG. 9. Influence of precipitating agent during Au deposition on Ti–MCM-48 (16 wt% Au in solution, Si/Ti = 50) on the epoxidation of propene at 150°C.

Au loading on cubic Ti–MCM-48 increases when the precipitating agent is changed from LiOH to CsOH. The worst performance of the catalyst occurring when CsOH is used to deposit gold may, therefore, be related to the highest gold loading. To run the reaction at higher temperature the decrease in both Au and titanium loadings is the most important parameter. We have also found that a pH of about 7.0 ± 0.1 works best to obtain the better performance of the catalyst in the propene epoxidation reaction (Fig. 10). This is most probably due to the higher dispersion of Au particles and the appropriate amount of Au loading on the support.

The results of the influence of Au loading in the catalyst Au/Ti–MCM-48 (Si/Ti = 50) on the epoxidation of propene at 150°C are given in Fig. 11. With an increase in Au loading, propene, H_2, and O_2 conversions increase whereas PO selectivity decreases. Propene conversion almost levels off at the 16% Au loading in the solution. The low Au loading of 2.0 wt% in the solution, which gave an actual loading of 0.01 wt% (Table 1), is also not good, as it is not sufficient to obtain a good yield. At the Au loading below 2 wt% in solution (0.01 wt% actual) formation of propane was observed. We reported earlier (39) that at the lower Au loading of $\leq$0.2 wt% propane formations occur over Au/TiO_2 due to the formation of Au particles smaller than 2 nm in diameter.

The results of the catalyst calcination temperature on the epoxidation activity are presented in Table 2. Propene conversion passes through a maximum for the catalyst calcined

TABLE 2

Influence of Catalyst Calcination Temperature on the Epoxidation of Propene

Temp. (°C) for		Conversion (%) of[c]			Selectivity (%) for	
Calcination[a]	Pretreatment[b]	C_3H_6	H_2	O_2	PO	CO_2
150	150	1.73	27.3	19.5	89	8.0
200	200	2.86	26.9	15.2	92	6.0
300	250	3.03	21.8	13.5	92	5.6
400	250	1.87	17.3	11.6	93	5.0
500	250	1.50	15.5	10.0	94	4.8

Note. Catalyst, 16 wt% Au/Ti–MCM-48 (Si/Ti = 50); reaction temperature, 100°C.

[a] In air.

[b] In 10 vol% O_2 in Ar.

[c] After 30 min of reaction.

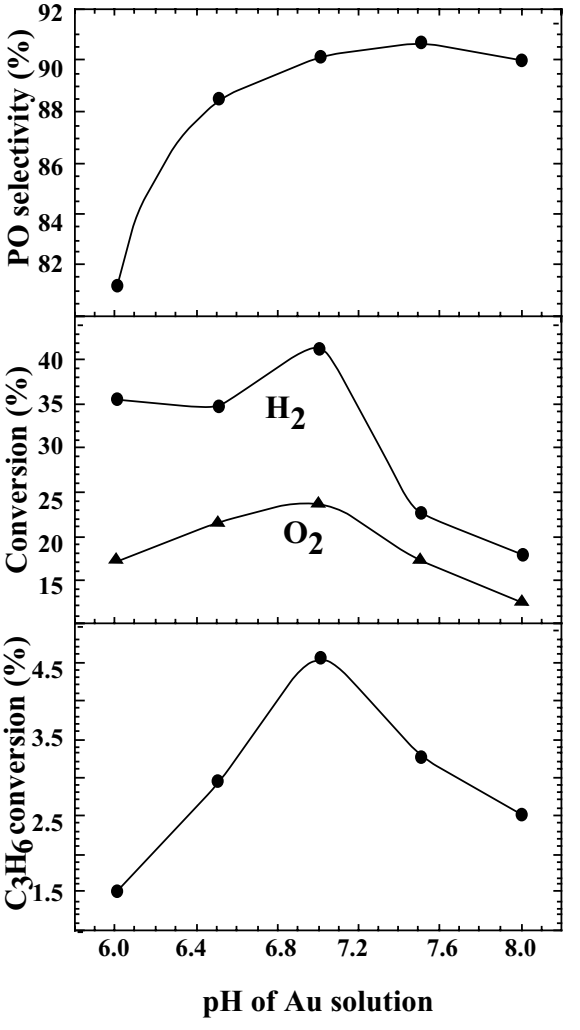

FIG. 10. Influence of pH during deposition of Au on Ti–MCM-48 (Si/Ti = 50) on the epoxidation activity at 150°C.

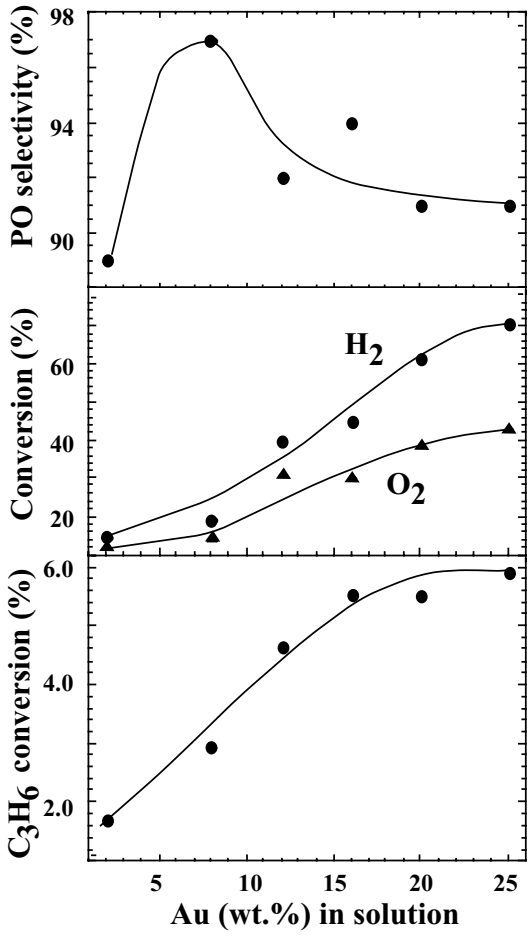

FIG. 11. Influence of Au content in DP solution in the catalyst Au/Ti–MCM-48 (Si/Ti = 50) on the epoxidation of propene at 150°C.

at 300°C. The increase in PO selectivity with an increase in catalyst calcination temperature is expected due to the stronger contact between the support, Ti–MCM-48, and the Au particles. The surprising fact is that even the catalyst calcined at 150°C produces PO with a propene conversion of about 1.7%. At such a low calcination temperature the reduction of $Au(OH)_3$ into its metallic state might not be completed. Our attempt to detect the presence of Au^+ and Au^{3+} species by XPS for the catalyst calcined at 150°C was unsuccessful due to highly dispersed Au particles, mostly inside the channels, even though the Au loading was very high. The results in the epoxidation of propene, however, may indicate that the reduction of $Au(OH)_3$ can take place easily during pretreatment and/or reaction due to the reducing atmosphere. The inferior performance of the catalyst calcined at 150°C can be correlated to the somewhat lower dispersion and bigger size of Au particles, as given in Table 1.

3.3. Catalysts Deactivation and Their Regeneration

A major problem associated with this system is the fast catalyst deactivation. The experimental results of the preadsorbed PO or propene on the catalysts before the start of the reaction suggests that the catalyst deactivation occurs mainly due to the adsorption of PO, not of propene. A GC-MS study indicated the presence of a large number of organic compounds adsorbed on the catalyst surface. These are acetic acid, propanoic acid, 1-acetoxy-2-propanol, 2-acetoxy-1-propanol, 1-hydroxy-2-propanone, propylene glycol, propylene carbonate, 2,5-dimethyl-1,4-dioxane, and so forth. We assume that these species are formed due to initial PO adsorption on the catalyst surface and its further oligomerization, rearrangement, cracking, coupling, and so forth, on the free titanium and acidic sites. As in the case of Ti/SiO_2 support (17), acidic species such as acetic acid and propanoic acid may also contribute to the catalyst deactivation. Earlier studies (40) on liquid-phase epoxidation of propene with H_2O_2 over TS-1 using methanol solvent shows that the major by-products responsible for catalysts deactivation, 1-methoxy-2-propanol and 2-methoxy-1-propanol, are formed from PO by epoxide ring opening and reaction with a nucleophile. It should be noted that the catalyst deactivation in liquid- and gas-phase epoxidation processes are caused by entirely different by-products, as mentioned above, thus suggesting different ways of catalyst deactivation in these two methods. Our attempts to regenerate the deactivated catalysts by thermal treatment at $\geq$250°C in the oxygen stream and also by dissolving organic moieties from the catalyst surface in organic solvents such as ethanol and acetone failed to recover the original activity of the catalysts. Nijhuis *et al.* (15) also indicated that the sequential oligomerization of propene oxide leading to species like dioxanes and heavier hydrocarbons may be the main cause of the lower epoxidation yield.

3.4. Silylation of Au/Ti–MCM-48

In the silylation process active hydrogen of silanol is replaced by an alkylsilyl group, making the material more hydrophobic. Corma and co-workers (40) showed earlier that the hydrophilic nature of Ti–MCM-41 makes it less active than Al–Ti–beta in aqueous H_2O_2 oxidation of alkanes and alkenes. Silylation using various volatile and easily removable silylating agents has improved hydrophobicity of Ti–MCM-41, resulting in large enhancement of epoxide yield, as reported in recent publications (42–44). In our study, silylation of the Au/Ti–MCM-48 performed using methoxytrimethyl silane improved PO selectivity and also substantially decreased H_2 consumption, but the initial propene conversion was also decreased (Fig. 12). The initial decrease in propene conversion could be related to the covering of active Au–Ti sites. It would be ideal if hydrogen was consumed on an equimolar basis to that of propene; however, due to higher temperature direct hydrogen oxidation takes place preferentially, resulting in low hydrogen efficiency. That silylation of the catalyst Au/Ti–MCM-48 results in the improvement of hydrogen consumption efficiency is a good sign and hence critical experiments are

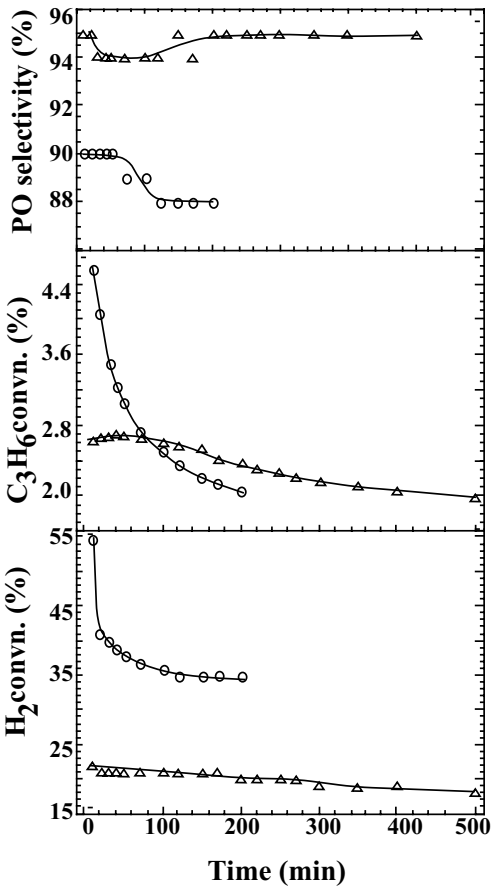

FIG. 12. Effect of trimethylsilylation of Au/Ti–MCM-48 catalyst on the propene epoxidation activity. Au in solution, 8 wt%; Si/Ti = 50; temperature = 150°C.

needed to make the commercial feasibility of this process more realistic.

3.5. Probable Reaction Mechanism

A theoretical prediction of Olivera *et al.* (44) suggests that the surface of gold is capable of generating H_2O_2. We have, therefore, proposed a probable reaction mechanism, as shown in Fig. 13, which is different from that

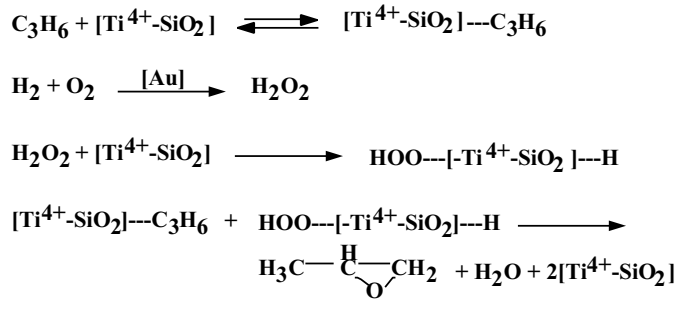

FIG. 13. Proposed reaction mechanism for propene epoxidation over Au/Ti–MCM catalysts.

which we proposed for Au/TiO_2 (12). Accordingly, hydrogen peroxide formed on the surface of gold would form hydroperoxolike species on the catalyst surface having isolated tetrahedral titanium sites. Hydroperoxolike species are expected to react with propene preadsorbed on the SiO_2 surface, giving PO formation by the same mechanism as reported for the liquid-phase epoxidation of propene using hydrogen peroxide (3). Moulijn and co-workers (15) proposed three different types of mechanisms and finally concluded that a hydroperoxidelike compound is more likely to be formed, creating a necessity for hydrogen. Our proposed mechanism is very similar to that recently proposed by Moulijn and co-workers (15). Detailed and critical experiments are needed in order to confirm the above mechanism.

4. CONCLUSIONS

1. XRD, UV–vis, FT-IR, and the very high surface area of above 1000 $m^2\ g^{-1}$ confirm the structural integrity and mesoporous nature of the supports Ti–MCM-41 (cubic) and Ti–MCM-48 (cubic). No segregated TiO_2 phase in the supports were observed and Ti was present as an isolated species in its tetrahedral coordination as long as the titanium content Si/Ti $\geq$ 50.

2. Finely dispersed Au with an average particle size of about 2–5 nm can be deposited homogeneously on both supports, using the DP method followed by calcination in air at 300°C.

3. The superior performance of Au/Ti–MCM-48 over that of Au/Ti–MCM-41 in the vapor-phase epoxidation of propene using H_2 and O_2 is attributed to its three-dimensional (cubic) pore system, which can be more resistant to blockage by extraneous materials like oligomers of PO and bulkier organic compounds, as evidenced in a GC-MS study, than the unidimensional pore system of hexagonal Ti–MCM-41.

4. In the case of Ti–MCM-48 support the best results are obtained when the following parameters are chosen: Si/Ti mole ratio = 50; precipitating agent = NaOH; Au loading (in solution) = 16 wt% (0.3 wt% actual); pH of the Au solution of 7.0 ± 0.1; calcination temperature of the catalyst = 300°C for 4 h in air; pretreatment conditions = 250°C for 30 min each, first in a flow of H_2 and then in O_2 (10 vol%), both diluted with argon; and reaction temperature =, 150°C.

5. Catalyst deactivation takes place not only due to the large number of organic compounds on the catalyst surface but also due to acidic compounds such as acetic acid.

6. Silylation helps improve PO selectivity and H_2 efficiency, probably due to an increase in the hydrophobicity of the catalyst.

7. A new reaction mechanism is proposed. Hydrogen peroxide formed from H_2 and O_2 over the gold surface is first converted into a hydroperoxolike species on the

Ti^{4+}–SiO_2 surface, which reacts with propene preadsorbed on the SiO_2 surface, giving PO.

ACKNOWLEDGMENTS

The authors are greatly indebted to Mr. T. Hayashi and Mr. Wada of Nippon Shokubai Co., Ltd., Japan, for their discussion and guidance in silylation technique. B.S. Uphade gratefully acknowledges the financial support of the Science and Technology Agency of Japan.

REFERENCES

1. Ainsworth, S. J., *Chem. Eng. News* 9 (1992).
2. van Santen, R. A., and Kuipers, H. P. C. E., *Adv. Catal.* **35**, 265 (1987).
3. Clerici, M. G., Bellussi, G., and Romano, U., *J. Catal.* **129**, 159 (1991).
4. Notari, B., *Catal. Today* **18**, 163 (1993).
5. Occhiello, E., *Chem. Ind.* 761 (1997).
6. Sato, A., Miyake, T., and Saito, T., *Shokubai* **34**, 132 (1992).
7. Meiers, R., Dingerdissen, U., and Hölderich, W. F., *J. Catal.* **176**, 376 (1998).
8. Haruta, M., *Catal. Surv. Jpn.* **1**, 61 (1997), and references therein.
9. Haruta, M., *Catal. Today* **36**, 153 (1997), and references therein.
10. Haruta, M., *Stud. Surf. Sci. Catal.* **110**, 123 (1997), and references therein.
11. Hayashi, T., Tanaka, K., and Haruta, M., *Shokubai* **37**, 72 (1995).
12. Hayashi, T., Tanaka, K., and Haruta, M., *J. Catal.* **178**, 566 (1998).
13. Kalvachev, Y. A., Hayashi, T., Tsubota, S., and Haruta, M., *Stud. Surf. Sci. Catal.* **110**, 965 (1997).
14. Haruta, M., Uphade, B. S., Tsubota, S., and Miyamoto, A., *Res. Chem. Intermed.* **24**, 329 (1998).
15. Nijhuis, T. A., Huizinga, B. J., Makkee, M., and Moulijn, *Ind. Eng. Chem. Res.* **38**, 884 (1999).
16. Stangland, E. E., Stavens, K. B., Andres, R. P., and Delgass, W. N., *J. Catal.* **191**, 332 (2000).
17. Mul, G., Zwijnenburg, A., van der Linden, B., Makkee, M., and Moulijn, J. A., *J. Catal.* **201**, 128 (2001).
18. Bowman, R. G., Clark, H. W., Maj, J. J., and Hartwell, G. E., PCT/US97/11414, PCT Pub. WO 98/00413.
19. Hayashi, T., Wada, M., Haruta, M., and Tsubota, S., Jpn. Pat. Pub. H10-244156, PCT Pub. WO97/00869, U.S. Patent 5,932,750.
20. Uphade, B. S., Tsubota, S., Hayashi, T., and Haruta, M., *Chem. Lett.* 1273 (1998).
21. Uphade, B. S., Okumura, M., Tsubota, S., and Haruta, M., *Appl. Catal. A* **190**, 43 (2000).
22. Uphade, B. S., Yamada, N., Nakamura, T., and Haruta, M., *Appl. Catal. A* **215**, 137 (2001).
23. Kresge, C. T., Leonowicz, M. E., Roth, W. J., Vartuli, J. C., and Beck, J. S., *Nature* **359**, 710 (1992).
24. Beck, J. S., Vartuli, J. C., Roth, W. J., Leonowicz, M. E., Kresge, C. T., Smith, K. D., Chu, C. T.-W., Olson, D. H., Sheppard, E. W., McCullen, S. B., Higgins, J. B., and Schlenker, J. L., *J. Am. Chem. Soc.* **114**, 10834 (1992).
25. Morey, M. S., Davidson, A., and Stucky, G. D., *J. Porous Mater.* **5**, 195 (1998).
26. Zhang, W., and Pinnavaia, T. J., *Catal. Lett.* **38**, 261 (1996).
27. Zhang, S. G., Fujii, Y., Yamashita, H., Tatsumi, T., and Anpo, M., *Chem. Lett.* 659 (1997).
28. Watanabe, K., Onoda, Y., Tsuneki, H., and Tatsumi, T., Jpn. Patent App. H07-300312.
29. Koyano, K. A., and Tatsumi, T., *Stud. Surf. Sci. Catal.* **105**, 93 (1997).
30. Haruta, M., Tsubota, S., Kobayashi, T., Kageyama, H., Genet, M. J., and Delmon, B., *J. Catal.* **144**, 175 (1993).
31. Corma, A., Navarro, N. T., and Perez-Pariente, J., *J. Chem. Soc. Chem. Commun.* 147 (1994).
32. Alba, M. D., Luan, Z., and Klinowski, J., *J. Phys. Chem.* **100**, 2178 (1996).
33. Koyano, K. A., and Tatsumi, T., *J. Chem. Soc. Chem. Commun.* 145 (1996).
34. Koyano, K. A., and Tatsumi, T., *Microporous Mater.* **10**, 259 (1997).
35. Hayashi, T., Wada, M., Haruta, M., and Tsubota, S., Jpn. Pat. Appl. H10-41833, PCT Pub. WO/JP99/00753.
36. Yuan, Z. Y., Liu, S. K., Chen, T. H., Wang, J. Z., and Li, H. X., *J. Chem. Soc. Chem. Commun.* 973 (1995).
37. Anpo, M., Yamashita, H., Ikeue, K., Fuji, Y., Zhang, S. G., Ichihashi, Y., Park, D. R., Suzuki, Y., Koyano, K., and Tatsumi, T., *Catal. Today* **44**, 327 (1998).
38. Tanaka, K., Hayashi, T., and Haruta, M., *J. Jpn. Inst. Metals* 547 (1996).
39. Thiele, G. F., and Roland, E., *J. Mol. Catal. A* **117**, 351 (1997).
40. Blasco, T., Corma, A., Navarro, M. T., and Pariente, J. P., *J. Catal.* **156**, 65 (1995).
41. Tatsumi, T., Koyano, K. A., and Igarashi, N., *Chem. Commun.* 325 (1998).
42. D'Amore, M. B., and Schwarz, S., *Chem. Commun.* 121 (1999).
43. Bu, J., and Rhee, H.-K., *Catal. Lett.* **65**, 141 (2000).
44. Olivera, P. P., Patrito, E. M., and Sellers, H., *Surf. Sci.* **313**, 25 (1994).